Optical Coherence Tomography in the Diagnosis of Skin Cancer

Amanda Levine, MD[a,b,c], Katie Wang, DO[a,b,c], Orit Markowitz, MD[a,b,c,*]

KEYWORDS

• Optical coherence tomography • Nonmelanoma skin cancer • Melanoma • Noninvasive imaging

KEY POINTS

- A review of the literature shows that optical coherence tomography (OCT) increases the overall sensitivity, specificity, and diagnostic accuracy compared with clinical and dermoscopy evaluation alone.
- Frequency Domain OCT (FD-OCT) has imaging depth of up to 2 mm, with enough cellular clarity to diagnose nonmelanoma skin cancers. Dynamic OCT (D-OCT) enables us to visualize vascular patterns in the skin, improving diagnostic accuracy. Finally, high-definition OCT (HD-OCT) has improved cellular resolution compared with FD-OCT and D-OCT, at the sacrifice of penetration depth and field of view. However, HD-OCT serves to fill the gap between reflectance confocal microscopy and conventional FD-OCT.
- OCT has also been shown to be useful in tumor margin delineation and is, thus, useful in preoperative treatment planning. In addition, OCT enables noninvasive treatment monitoring of skin cancers undergoing nonsurgical therapies.

INTRODUCTION

Over the past decade, optical coherence tomography (OCT) has emerged as a novel noninvasive imaging device that allows for the real-time, in vivo, cross-sectional imaging of skin morphology. The advantage of these noninvasive devices over histopathology is that they enable repeated imaging of the same unaltered skin sites to observe dynamic events and long-term changes over time. Therefore, OCT has been used in both clinical and research settings to aid in the diagnosis of clinical and subclinical lesions; delineate lesion margins; and, unique to OCT given its larger field of view (FOV) and increased depth, monitor lesions undergoing nonsurgical treatment.

OPTICAL COHERENCE TOMOGRAPHY

OCT imaging is based on low-coherence interferometry to detect the intensity of backscattered infrared light from biological tissues by measuring the optical path length.[1–4] With these imaging devices, there is an inverse relationship between cellular clarity and both FOV as well as depth.[1] Basically, as imaging depth and lateral resolution increases, the cellular resolution decreases (**Table 1**).

Disclosure Statement: Dr O. Markowitz is an investigator for Michelson Diagnostics and Caliber ID. Dr A. Levine and Dr K. Wang have nothing to disclose.

[a] Department of Dermatology, SUNY Downstate Medical Center, 450 Clarkson Avenue, Brooklyn, NY 11203, USA; [b] Department of Dermatology, New York Harbor Healthcare System, 800 Poly Place, Brooklyn, NY 11209, USA; [c] Department of Dermatology, Mount Sinai Medical Center, 5 East 98th Street, New York, NY 10029, USA

* Corresponding author. 5 East 98th Street, New York, NY 10029.
E-mail address: omarkowitz@gmail.com

Dermatol Clin ■ (2017) ■–■
http://dx.doi.org/10.1016/j.det.2017.06.008

Table 1
Summary of noninvasive imaging devices

Imaging Modality	Imaging Depth (mm)	Lateral Resolution (μm)	Axial Resolution (μm)	FOV (mm)	Probe Aperture Size
RCM	0.2	0.5–1.0	3–5	0.5 × 0.5	3.16 cm
HD-OCT	0.57	3	3	1.8 × 1.5	5 cm
FD-OCT, D-OCT/ SV-OCT	1.5–2.0	7.5	5	6.0 × 6.0	1.38 cm
HFUS (20 MHz)	10	200	80	12	10–20 mm

Abbreviations: D-OCT, dynamic OCT; FD-OCT, Frequency Domain OCT; HD-OCT, high-definition OCT; HFUS, high-frequency ultrasound; RCM, reflectance confocal microscopy; SV-OCT, speckle variance OCT.

There are several different OCT imaging modalities that have been studied. The swept-source multi-beam Frequency Domain OCT (FD-OCT) (Vivosight, Michelson Diagnostics, Kent, United Kingdom) provides 2 real-time imaging modes: b-scan (vertical, cross-sectional), similar to histology, and en face modes (horizontal), similar to that of dermoscopy and reflectance confocal microscopy (RCM). The images have an optical resolution of less than 7.5 μm laterally and less than 5 μm axially, a penetration depth of up to 2 mm, and an FOV of 6.0 mm × 6.0 mm.[1–4] A recent advancement, dynamic OCT (D-OCT) based on speckle variance OCT (SV-OCT), allows for visualization of skin microvasculature and the detection of blood flow.[1] Angiogenesis is important in the growth and spread of cancers; thus, visualization of vessel morphology is helpful in improving diagnostic accuracy.

Although conventional FD-OCT has been shown to be useful in skin imaging, its limited resolution precludes visualization of the skin at the cellular level. High-definition OCT (HD-OCT) (Skintell device, Agfa Healthcare, Mortsel, Belgium) seems to bridge the gap between conventional FD-OCT imaging and RCM offering improved axial and lateral resolution of 3 μm, with the trade-off of a more limited penetration depth of about 750 μm and FOV of 1.8 mm × 1.5 mm.[1–4]

High-frequency ultrasound is another imaging modality that has the largest penetration depth and FOV, however, lacks the cellular resolution necessary for skin visualization (<1 mm) and is, therefore, not frequently used in the diagnosis and management of skin.[5]

When comparing the different imaging methods, it is important to be aware of the imaging mode. FD-OCT, D-OCT, and HD-OCT devices all provide both vertical and horizontal en face images, creating a 3-dimensional image.[2–4] The vertical scans are helpful in that they mimic histology sections; the horizontal view, similar to RCM, helps bridge the gap of dermoscopy to histology.

Another parameter to consider is the probe aperture size to FOV ratio. Noninvasive devices have a probe that directly touches the skin and produces an image based on its FOV. Usually the FOV is much smaller than the probe itself. The smaller the aperture and the larger the FOV the less of a discrepancy between what the probe comes in contact with and what is actually being imaged. Thus, a smaller variation in the aperture to FOV ratio leads to more accurate probe placement and, therefore, a better correlation of what you are imaging and what you see clinically. This smaller variation is especially important at varying time points if, for example, you are monitoring a lesion undergoing treatment. Additionally, a small probe can be positioned to image in more cosmetically sensitive areas, such as the head and neck. Ultrasound has the best FOV to aperture size ratio followed by FD- and D-OCT as seen in **Table 1**.

FREQUENCY DOMAIN-OPTICAL COHERENCE TOMOGRAPHY

FD-OCT has mainly been used in the cross-sectional (vertical mode) similar to histology (**Table 2**).

Basal Cell Carcinoma

There have been several studies investigating the accuracy of FD-OCT in diagnosis of basal cell carcinoma (BCC). The literature indicates that FD-OCT increased sensitivity, specificity, and diagnostic accuracy compared with clinical and dermoscopy assessment alone.[6–11] There are few studies showing that FD-OCT is able to distinguish between the different BCC subtypes.[7–9] However, some studies think FD-OCT lacks the cellular clarity to make this distinction.

The major diagnostic criteria on FD-OCT for BCC are alteration of the dermoepidermal junction (DEJ) and dark ovoid basal cell islands in the dermis, which are typically surrounded by a darker, hyporeflective peripheral border.[6–11] Often

Table 2
Frequency Domain

First Author, Year, Country	Population Characteristics	Lesions, Number	Accuracy	Findings/Results	Limitations
Maher et al,[28] 2016, Australia	88 patients (47 M, 28 F), mean age 63 y	88 equivocal amelanotic or hypomelanotic skin lesions (AHM = 13), mostly located on the trunk (n = 36), lower limb (n = 16), upper limb (n = 18), head/neck (n = 18)	NR	OCT features of icicles and dermal ovoid structures with dark borders both significant (P<.05) for diagnosis of AHM compared with other study lesions DEJ disruption commonly seen in AHM on OCT (10 of 13 cases) but was also seen in other NMSC, thus, lacked specificity	Limited number of significant OCT features to help identify AHM because OCT only provides architectural, superficial view of a skin lesion but does not offer cellular resolution Weak inter-rater agreement
Markowitz et al,[30] 2016, United States	30 male patients, aged 67–93 y (mean 76 y), all being treated with ingenol mebutate gel 0.015%; 2 patients excluded	336 lesions (168 clinical AKs, 168 perilesional)	OCT detected 100% (28 of 28) of clinical and 73% (16 of 22) of subclinical lesions at baseline	At day 60, OCT indicated 76% clinical lesion clearance rate (52 of 68) for ingenol mebutate treated areas vs 11% (6 of 55) for untreated areas Clearance rate for subclinical lesions with ingenol mebutate: 88% (21 of 24) vs 43% (6 of 14)	Only 28 subjects, all of whom represented a very similar demographics OCT scans read by single blinded dermatologist

(*continued on next page*)

Table 2
(*continued*)

First Author, Year, Country	Population Characteristics	Lesions, Number	Accuracy	Findings/Results	Limitations
Cheng et al,[8] 2016, Australia	103 patients (63 M, 40F), aged 31–88 y (median 66 y)	168 lesions: 52% sBCC, 26% other BCC variants, remainder were AK, SCCIS, other benign inflammatory processes and 2 other malignant tumors Lesions located on the trunk (55.4%), upper extremity (18.5%), head/neck (13.7%), lower extremity (12.5%)	sBCC diagnosis Sensitivity 87%, specificity 80%, PPV 83%, NPV 86% With high clinical confidence for sBCC (>90%), and high OCT interpreter confidence, an accuracy rate of 89% Interobserver agreement: 3 observers of varying experience, $\kappa = 0.596$; among 2 experienced observers, $\kappa = 0.766$	Clefting, hyporeflective ovoid structure, and absence of a fully encompassing ovoid structure highly predictive of sBCC Good diagnostic accuracy with OCT for diagnosing sBCC and measuring depth in tumors <0.4 mm Potential to reduce the need for biopsy in clinically suspected sBCCs with OCT use; careful follow-up required as there is a small risk (5%) of misdiagnosis; a potential 76% biopsy reduction rate of biopsy associated with a 5% error rate Good interobserver agreement between experienced and inexperienced observers	Potential pitfall: identified case of amelanotic melanoma that was diagnosed as sBCC clinically and on OCT
Meekings et al,[9] 2016	NR	40 BCCs (13 nodular, 22 superficial, 5 morpheaform)	NR	Diagnostic criteria for BCC: hyporeflective ovoid structures (40 of 40), dark halo boundaries (38 of 40), epidermal thinning (28 of 40), and collagen compression (14 of 40)	Retrospective study Unblinded interpreters

Olsen et al,[10] 2016, Denmark	162 patients (90 M, 73 F), mean age 69.4 y	142 lesions (41 BCCs, 30 AKs, 71 normal skin) located mainly on the head (90 of 142), followed by the trunk (32 of 142) and extremities (20 of 142)	Skilled observers: Diagnosing AK: sensitivity 56%–96%, specificity 52%–83% Diagnosing BCC: sensitivity 86%–95%[a], specificity 81%–98%[a] Diagnosing healthy skin: sensitivity 36%–84%[a], specificity 95%–100% Differentiating NMSC vs healthy skin: sensitivity 94%–100%, specificity 28%–76% Unskilled observers: Diagnosing AK: sensitivity 54%–83%, specificity 52%–65% Diagnosing BCC: sensitivity 66%–85%, specificity 73%–94% Diagnosing healthy skin: sensitivity 20%–52%, specificity 94%–100% Differentiating NMSC vs healthy skin: sensitivity 93%–100%, specificity 21%–54%	Note: skilled observers: 1–10 y of OCT research and 3–28 y clinical experience in dermatology; unskilled observers: no experience in OCT and 1–15 y of clinical experience in dermatology Skilled observers better at interpreting OCT images compared with unskilled observers with a significantly higher sensitivity and specificity in diagnosing BCC and healthy skin; thus, potential increase in diagnostic accuracy with intensified training in OCT For AK: no significant difference in sensitivity or specificity between groups	NMSC lesions overdiagnosed by both groups: resulting in high sensitivity but a mediocre specificity and may be because OCT images of healthy skin were obtained from skin adjacent to NMSC lesions and, thus, may have features of sun damage due to field cancerization Study based on selected good-quality OCT images without significant artifacts from hairs and hyperkeratotic areas: not representative of population
Wahrlich et al,[29] 2015, Germany	130 patients (58 F, 72 M), average age 68.1–61.3 y	98 BCCs, located on the head, trunk, extremities, 29 other skin diseases	Application of scoring system, Berlin Score Students: sensitivity 92.8%, specificity 24.1% Experts: sensitivity 96.6%, specificity 75.2%	88% of all diagnoses correctly classified & confirmed by histopathology	Invasive SCC most frequent false-positive diagnosis

(*continued on next page*)

Table 2
(*continued*)

First Author, Year, Country	Population Characteristics	Lesions, Number	Accuracy	Findings/Results	Limitations
Maier et al,[12] 2015, Germany	4 patients (3 F, 1 M)	14 AK lesions located on the upper extremity undergoing topical ingenol mebutate	NR	OCT features of AK pretreatment: crusts or scaling, epidermal broadening and thickening, ill-defined dermoepidermal boarder, hyperkeratosis During treatment: subepidermal blistering, dermal edema Noninvasive imaging superior to clinical evaluation to detect nonresponding lesions	Case series
Ulrich et al,[7] 2015, Germany	156 patients, aged 33–90 y (median 70 y)	Total: 235 nonpigmented pink lesions suspicious for BCC Histology identified 141 of 235 (60%) as BCCs (44 nBCC, 59 sBCC, 19 sclerosing BCC, 19 other BCC), located mostly on head (41.0%) and upper body (48.8%)	Increase in sensitivity from 90.0% (clinical examination) to 95.7% (clinical + dermoscopy + OCT) (P = .099) Increase in specificity from 28.6% by clinical assessment to 54.3% using dermoscopy and to 75.3% with the addition of OCT (P<.001)[a] PPV: 66.0% (clinical), 75.0% (dermoscopy), 85.2% (OCT) NPV: 65% (clinical), 79.4% (dermoscopy), 92.1% (OCT)	Diagnostic accuracy: increase from 65.8% (clinical) 76.2% (clinical + dermoscopy) to 87.4% (clinical + dermoscopy + OCT)	Caution for rare cases of amelanotic melanoma, which can present as a pink patch, plaque, or nodule

Blumetti et al,[13] 2015, Brazil	NR	39 lesions: 19 melanomas (10 in situ, 9 invasive, with Breslow thickness <1 mm), 15 compound nevi, 5 junctional nevi	NR	Presence of dermal shadows correlated significantly with in situ melanoma (8 in 10 cases, $P = .007$); shadows and loss of bright collagen correlated with invasive melanoma, compared with compound nevi ($P = .002$ and $P<.001$). Hyporeflective band associated with compound nevi (80%) and less frequently found in melanomas (31.5% $P = .007$) Summary: Prescience of dermal shadows and absence of bright collagen most relevant parameters to suggest malignancy Lack of hyporeflective bands on invasive melanomas distinguished this from compound nevi	Small population

(*continued on next page*)

Table 2
(*continued*)

First Author, Year, Country	Population Characteristics	Lesions, Number	Accuracy	Findings/Results	Limitations
Markowitz et al,[6] 2015, United States	100 patients, >18 y old	115 clinically challenging BCCs located on the head or neck	Diagnostic accuracy: 57.4% (clinical), 69.6% (dermoscopy), 87.8% (OCT) Increase in specificity from 48.9% by clinical assessment to 55.6% using dermoscopy and to 80% with the addition of OCT Increase in sensitivity from 62.9% by clinical assessment to 78.6% using dermoscopy and to 92.9% with the addition of OCT PPV: 65.7% (clinical), 74.3% (dermoscopy), 87.8% (OCT) NPV: 45.8% (clinical), 62.5% (dermoscopy), 87.8% (OCT)	Significant improvement in sensitivity and specificity over clinical or dermoscopic evaluation alone with OCT Certainty of diagnosis increased by OCT, with a positive effect on accuracy: increase in accuracy of diagnosis with OCT from 88% to 96% when diagnostic certainty was accounted for	Observational study involving only clinically difficult lesions and, thus, likely underestimates the specificity for obvious lesions
Mogensen et al,[37] 2009, Denmark	104 patients, mean age 69.3 y	64 BCCs, 1 baso-squamous carcinoma, 39 AKs, 2 malignant melanomas, 9 benign lesions Locations NR	Sensitivity 79%–94%, specificity 85%–96% for all NMSCs depending on experience		Error rate of 50%–52% with discrimination of AK from BCC, much higher than any other study, likely due to older OCT
Gambichler et al,[14] 2007, Germany	75 patients (42 M, 33 F), aged 15–95 y (mean 54.4)	92 melanocytic lesions (52 BN, 40 MM), mostly located on the trunk, followed by limbs and head.	NR	OCT of MM: marked architectural disarray and DEJ; large, vertical, icicle-shaped structures	Conventional OCT: not enough clear-cut differences demonstrated between MM and BN to be used

[a] Indicates statistical significance.

Abbreviations: AHM, amelanotic/hypomelanotic melanoma; AK, actinic keratosis; BCC, basal cell carcinoma; BN, benign nevi; DEJ, dermoepidermal junction; F, female; FD-OCT, frequency domain optical coherence tomography; M, male; MM, malignant melanoma; NMSC, nonmelanoma skin cancer; NPV, negative predictive value; NR, not reported; PPV, positive predictive value; sBCC, superficial basal cell carcinoma; SCCIS, squamous cell carcinoma in situ.

these ovoid structures are surrounded by a bright fibrous tumor stroma.[6–11] Additional features described include absence of normal hair follicles and glands as well as prominent dilated vessels in the superficial dermis directed toward the basaloid cell islands.[6–11] Some lesions also have small, well-circumscribed, black/hyporeflective areas inside the tumor nests, representing tumor necrosis (**Fig. 1**).[11]

Squamous Cell Carcinoma/Actinic Keratosis

Actinic keratosis (AK) is considered to be the initial lesion in a continuum that progresses to invasive squamous cell carcinoma (SCC). While clinically it can be difficult to distinguish between AK and SCC, the distinction is critical in determining appropriate treatment. The use of noninvasive imaging can both improve diagnostic accuracy as well as increase the detection of early subclinical disease states.

On FD-OCT, AKs appear as white streaks in the upper epidermis, indicated by hyperechogenic areas that correspond to hyperkeratotic scale.[10,12] There is thickening of the epidermis with a haphazard pattern in the upper portion, disruption of the normal layered skin architecture as well as ill-defined borders at the DEJ.[10,12] Compared with AKs, SCCs tend to have more epidermal thickening and haphazard patterning and appear more broadly throughout the FOV (**Figs. 2** and **3**).[10,12]

Melanoma

Compared with nonmelanoma skin cancer (NMSC), there are only a few studies investigating the use of OCT in pigmented lesions. Studies determined that conventional OCT did not demonstrate enough differences from benign nevi to be used as a diagnostic tool for malignant melanoma (MM).[13,14]

DYNAMIC OPTICAL COHERENCE TOMOGRAPHY

Basal Cell Carcinoma

On dermoscopic examination, the finding of arborizing vessels is a key feature in the diagnosis of BCC (**Table 3**). Thus, D-OCT has increased the sensitivity in diagnosing BCCs as it can look at the pattern and distribution of vessels.

On the cross-sectional view, BCCs demonstrate a progressive elongation of perpendicular vessel columns.[15–17]

In the en face view, the blood vessels appear irregular and disorganized, displaying a wide variation in blood vessel caliber.[15–17] In addition, BCCs display a high vessel density both throughout the lesion as well as lining the periphery of the tumor

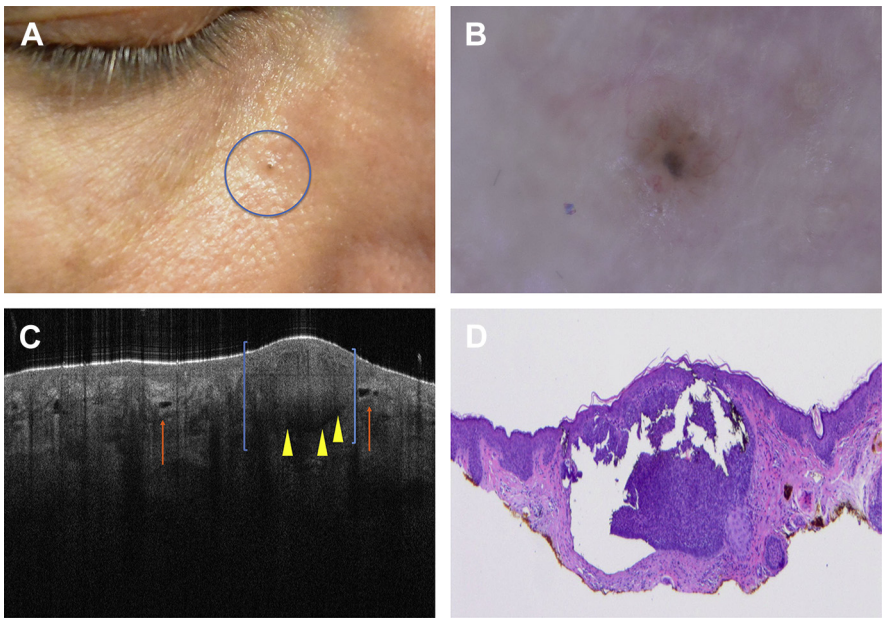

Fig. 1. Clinical, dermoscopy, FD-OCT, and histology of a BCC. (*A*) Clinical image of a BCC, appearing as a small pigmented papule (*blue circle*). (*B*) Dermoscopy of a pigmented BCC exhibiting brown/gray ovoid nest surrounded by barbarized vessels. (*C*) Cross-sectional FD-OCT image of a BCC. Features include dark hyporeflective ovoid area (*blue brackets*) with a black rim (*arrowheads*). Note the effaced DEJ above the BCC and the prominent blood vessels in the dermis (*orange arrows*). (*D*) Corresponding histopathology (Haemotoxylin and Eosin).

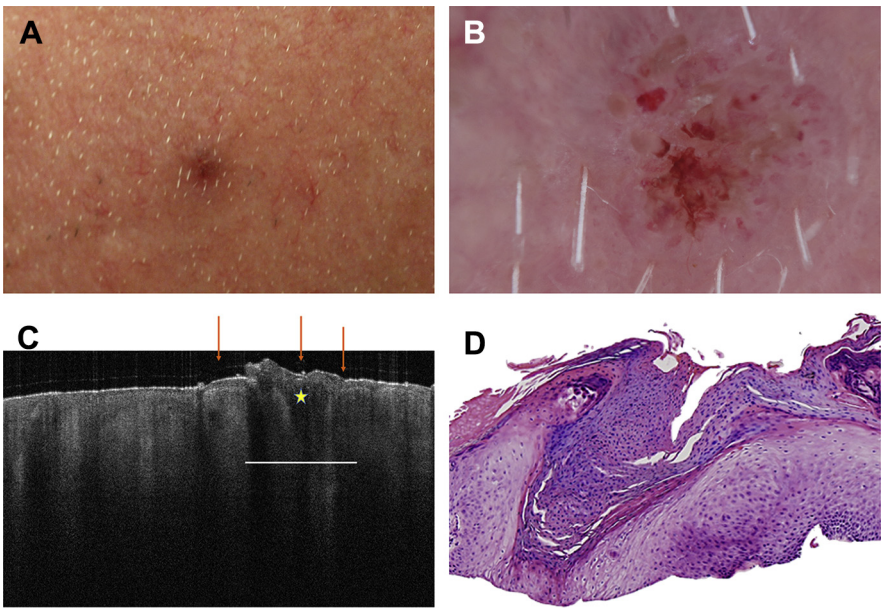

Fig. 2. Clinical, dermoscopy, FD-OCT, and histology of an AK. (*A*) Clinical image of an AK appearing as an erythematous, scaly, papule. (*B*) Dermoscopy shows minimal ulceration, some dotted vessels, and a superficial white hyper-reflective scale. (*C*) Cross-sectional FD-OCT image of an AK. Features include localized foci of epidermal thickening (*yellow star*) and hyperkeratotic scale (*orange arrows*). Note the disruption of the DEJ beneath the thickened epidermis. (*D*) Corresponding histopathology (Haemotoxylin and Eosin).

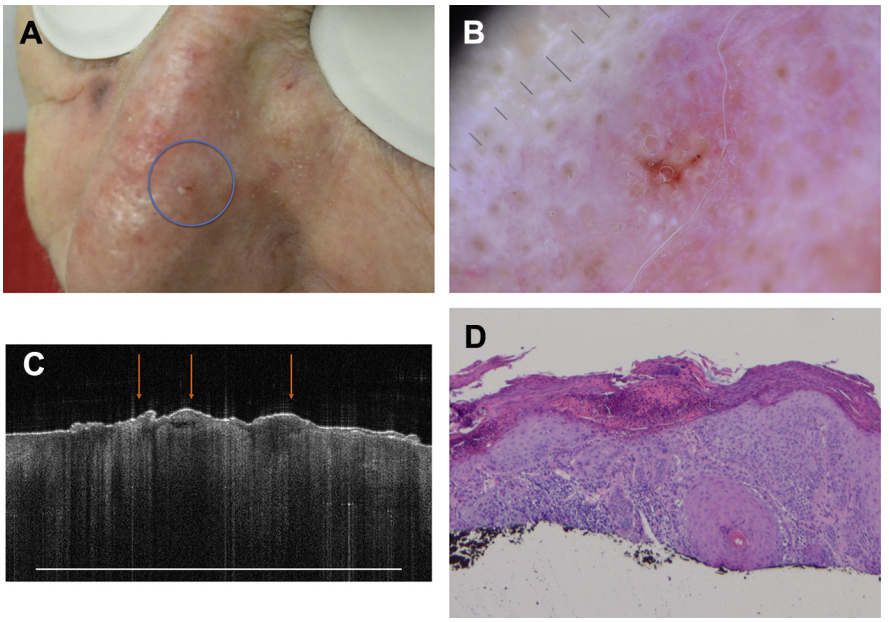

Fig. 3. Clinical, dermoscopy, FD-OCT, and histology of an SCC. (*A*) Clinical image of SCC appearing as a small erythematous, scaly papule (*blue circle*). (*B*) Dermoscopy shows ulceration with white hyper-reflective scale. (*C*) Cross-sectional FD-OCT image of an SCC. SCCs appear similar to that of actinic keratosis, although they exhibit more epidermal thickening and hyperkeratotic scale (*orange arrows*). They also appear more broadly throughout the FOV. Note the lack of a distinct DEJ. (*D*) Corresponding histopathology (Haemotoxylin and Eosin).

Table 3
Summary of studies investigating the use of optical coherence tomography to evaluate skin cancers: high-definition optical coherence tomography (Skintell)

First Author, Year, Country	Population Characteristics	Lesions, Number	Accuracy	Findings/Results	Limitations
Marneffe et al,[24] 2016, Belgium	36 patients (19 F, 17 M), aged 38–89 y (median 68 y)	106 lesions (38 AKs, 16 SCCs, 52 normal skin sites), localized mostly on the head/neck region and lower limbs	Experienced user: AK diagnosis: sensitivity 81.6%, specificity 92.6%, PPV 86.1%, NPV 90% SCC diagnosis: sensitivity 93.8%, specificity 98.9%, PPV 93.8%, NPV 98.9% Normal skin diagnosis: sensitivity 92.3%, specificity 88.9%, PPV 88.9%, NPV 92.3% All aforementioned listed numbers: consistently and statistically significantly higher than less-experienced observers	Disrupted DEJ: highly sensitive for invasive SCC, minimizing the false-negative rate Budding/periadnexal collars: enabled ~100% specificity for SCC, minimizing false-positive rate	Hyperkeratotic AKs, thought to be most likely to progress to SCC, excluded from this study because the high refractive index of the keratin interfered with the visualization of the deeper cutaneous layers Results obtained by 3 observers, cannot be extended to all dermatologists Only AKs and SCCs included in the study: did not evaluate discrimination from other diagnosis characterized by dyskeratosis (ie, psoriasis, lichen planus)

(*continued on next page*)

Table 3
(*continued*)

First Author, Year, Country	Population Characteristics	Lesions, Number	Accuracy	Findings/Results	Limitations
Boone et al,[23] 2015, Belgium	53 patients (25 M, 28 F), age 38–93 y (mean age 65.5 y)	53 lesions (37 AKs and 16 SCCs), 40 lesions on face, 9 extremities, 4 on the trunk	See Findings/Results	Discriminating SCC from AK and normal skin: Presence of outlined DEJ on cross-sectional imaging suggestive for normal skin or AK vs blurred/not detectable junction suggestive of SCC Sensitivity 100%, specificity 94% Discriminating AK from normal skin: En face mode: atypical honeycomb pattern (sensitivity 100%, specificity 100%); cross-sectional mode: alternating hyperkeratosis/parakeratosis (100% sensitivity, 100% specificity) Discriminating AKs with/without adnexal involvement: En face mode: presence and absence of the *cocarde* image distinguished AKs without from with adnexal involvement, respectively	Study does not represent a testing set but only a training set Severe hyperkeratotic (>300 μm) lesions excluded due to unclear visualization on HD-OCT; HAK important differential for invasive SCC, so further studies need to be done

Boone et al,[18] 2015, Belgium	50 patients (22 M, 28 F), range from 35 to 87 y (median 66 y)	50 BCCS: 18 sBCC, 19 nBCC, and 13 iBCC, located mainly on the trunk (62%), followed by head/neck (26%) and limbs (12%) 50 non-BCC (25 AKs, 12 melanocytic lesions, 10 sebaceous hyperplasias, 3 hemangiomas)	NR	Gray to dark lobulated structures present in 48 of 50 (96%) BCCs, in none of the AKs, and in all other BCC imitators; lobular structures characterized by a cockade feature (bright outer rim) in 37 of 50 (74%) BCCs and also present in 6 of 10 (60%) of sebaceous hyperplasias, but absent in other BCC imitators sBCC: lobular structures connected to the epidermis (swallow nests), type A vessels (short fine holes), absence of stretched fibers nBCC: lobular structures, stretched fibers, type B vessel (small branched holes) iBCC: lobular structures, stretched fibers, type C vessels (large branched holes)	
Gambichler et al,[25] 2015, Germany	64 patients	Total 93 melanocytic lesions: 66 BN (23 compound nevi, 20 JN, 10 dermal nevi, 9 DN, 2 nevoid lentigo, 2 blue nevi) and 27 melanomas (23 superficial spreading, 2 LMM, 1 nodular, 1 acral lentiginous melanoma)	HD-OCT for MM: sensitivity 74.1%, specificity 92.4%, PPV 80%, NPV 89.7%	HD-OCT risk parameters for MM: large roundish pagetoid cells, atypical cell clusters in DEJ, totally disarranged epidermal/dermal pattern, bright bizarre dermal horizontal streaks, large vertical icicle-shaped structures HD-OCT has moderate diagnostic potential in differentiating benign vs malignant MSL, however, is inferior to RCM	High false-negative rates in very thin melanomas and high false positive rates in dysplastic nevi Small sample size Only one blinded observer Used preliminary micromorphologic HD-OCT features of MSL

(*continued on next page*)

Table 3
(*continued*)

First Author, Year, Country	Population Characteristics	Lesions, Number	Accuracy	Findings/Results	Limitations
Boone et al,[26] 2014, Belgium	26 patients	26 melanocytic lesions (3 JN, 8 compound nevi, 1 DN, 1 blue nevus, 9 dysplastic nevi, 4 melanoma)	NR	HD-OCT melanoma: Cross-sectional mode: atypical large melanocytes in the upper part of the acanthotic epidermis, altered DEJ with irregular and broadened rete ridges, atypical cells tended to for junctional sheets or irregular junctional aggregates distorting the rete ridges En face mode: cobblestone or irregular honeycomb pattern in superficial layer, epidermal disarray in areas of pagetoid spread, atypical melanocytes in the upper part of dermis	Pilot study, small number of lesions
Gambichler et al,[27] 2014, Germany	n = 48	NR	NR	Showed that pagetoid cells, fusion of rete ridges, and junctional and/or dermal nests with atypical cells significantly more frequently seen in melanoma when compared with benign nevi Because of higher resolution: HD-OCT has higher diagnostic potential in differentiating between benign and malignant melanocytic lesions compared with conventional OCT	Absence of suspicious HD-OCT features in some thin melanomas is a major limitation of HD-OCT

Li et al,[19] 2014, Germany	43 patients (25 M, 18 F), aged 38–87 y (mean 65.3 y)	43 total lesions: 22 BCC, 10 fibrous papules of the face, 5 AK, 3 intradermal nevi, 2 SCC, 1 sebaceous hyperplasia	Experienced investigator diagnosing BCC: sensitivity of 86.4%, specificity of 90.5% Inexperienced investigator diagnosing BCC: sensitivity 77.3%, specificity 81%	Good interobserver agreement between experienced and inexperienced investigators (concordance of 77% and 81%, respectively)	
Gambichler et al,[20] 2014, Germany	20 patients (15 M, 5 F), mean age 67.1 y	25 BCCs (13 solid type, 9 superficial type, 3 infiltrative type)	NR	En face mode: lobulated nodules were seen in 21 of 25 lesions (84%, $P = .0014$), peripheral rimming in 18 of 25 (72%, $P = .046$), epidermal disarray 18 of 25 (72%, $P = .046$) and variably refractile stroma in 22 BCCs (88%, $P = .0003$) Cross-section: destruction of layering in 19 of 25 BCCs (76%, $P = .0164$)	Unable to differentiate different BCC subtypes
Maier et al,[21] 2013, Germany	14 M patients, aged 51–82 y	22 BCCs (11 nodular, 5 superficial, 4 infiltrative, 1 pigmented, 1 adenoid)	NR	En face mode: lobulated nodules (20 of 22), peripheral rimming (17 of 22), epidermal disarray (21 of 22), dilated vessels (11 of 22), and variably refractile stromal (19 of 22) Slice mode: gray/dark oval structures (18 of 22), peripheral rimming (13 of 22), destruction of layering (22 of 22), dilated vessels (7 of 22), peritumoral bright stroma (11 of 22)	

Abbreviations: BN, benign nevi; DN, dysplastic nevi; F, female; HAK, hypertrophic actinic keratosis; iBCC, invasive BCC; JN, junctional nevi; LMM, lentigo maligna melanoma; M, male; MSL, melanocytic skin lesions; nBCC, nodular BCC; NPV, negative predictive value; PPV, positive predictive value; sBCC, superficial BCC; SES, skin entrance signal.

islands, demarcating the tumor from normal skin (**Figs. 4** and **5**).[15–17]

Squamous Cell Carcinoma/Actinic Keratosis

On the en face view, AKs generally appear as a reticular network of vessels similar to normal skin, although tend to be slightly broader and more irregular.[15] In contrast, SCCs appear significantly different as regularly distributed dotted structures immediately below the epidermis (**Figs. 6** and **7**).[15]

Malignant Melanoma

Examining the vasculature of melanocytic lesions with D-OCT in the en face view has been shown to be useful in differentiating benign from malignant lesions. Congenital nevi usually display a pattern of regularly distributed dotted structures immediately below the epidermis, with a pattern usually comparable with surrounding skin.[15] In contrast, melanoma shows densely clustered red dots in the superficial dermis that present a chaotic and irregular vascular distribution compared with nevi.[15] As tumor thickness increases, the red dots aggregate to long linear vessels with angulated branches and irregular size (**Fig. 8**).[15–17]

HIGH-DEFINITION OPTICAL COHERENCE TOMOGRAPHY

Basal Cell Carcinoma

HD-OCT has improved cellular resolution compared with conventional FD-OCT and has been shown to not only correctly identify BCCs from its clinical imitators but also distinguish between different BCC subtypes (**Table 4**).

On en face mode, BCCs exhibit lobulated nodules, peripheral rimming, epidermal disarray, and variably refractile stroma.[18–21] On cross-sectional mode, BCCs have destruction of layering.[18–21]

Boone and colleagues[18] determined that the appearance of gray to dark lobulated structures with a bright outer rim (cockade feature), on both en face and cross-sectional imaging modes, were present in almost all BCCs and are, thus, considered the hallmark for diagnosis.[18] These lobular structures were absent in all AKs; although present in other BCC imitators, only sebaceous hyperplasias were found to also have a bright outer rim.[18] When the lobular structures were connected with a hair follicle, this was found to be pathognomonic of sebaceous hyperplasia and is one way to differentiate them from BCC.[18] All BCCs had increased vascularization within the superficial papillary dermis, displayed as holes on HD-OCT, although the appearance differed between subtype.

BCC subtype could be classified based on the type of lobular structures, the presence or absence of stretched fibers in the stroma (stretching effect), and the dominant vascular pattern present.[18]

Superficial BCCs (sBCCs) were the only BCC subtype to have lobular structures directly connected to the epidermis (swallow nests), type A vessels (short, fine holes), and the absence of stretched fibers (**Figs. 9** and **10**).[18] In contrast, nodular BCCs (nBCCs) and invasive BCCs (iBCCs) had lobular structures with cockade not connected to the epidermis and almost all of them

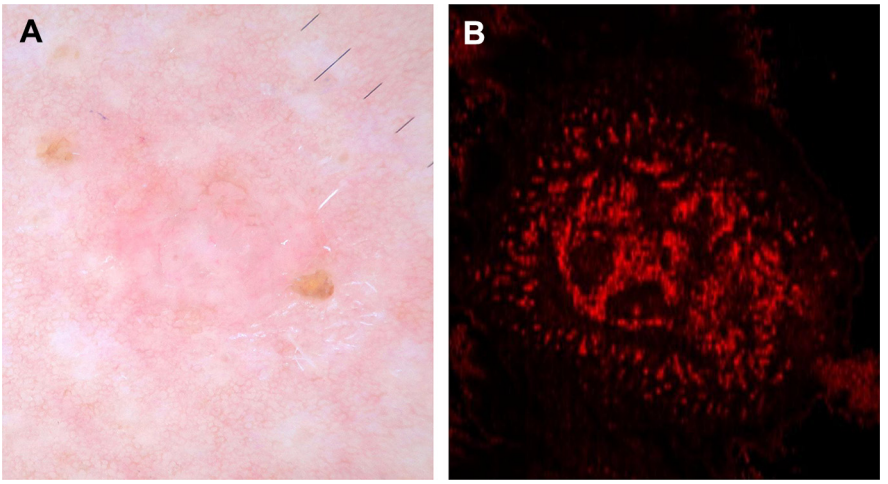

Fig. 4. Dermoscopy and en face view of BCC on D-OCT: (*A*) Dermoscopy of BCC with pink-white shiny background, focal ulceration, arborizing vessels. (*B*) En face D-OCT of BCC shows disarray of thin, irregular vessels that are variable in size compared with the normal facial vessels. In comparison with more aggressive tumors, such as melanoma, the vascular pattern appears confined to the tumor.

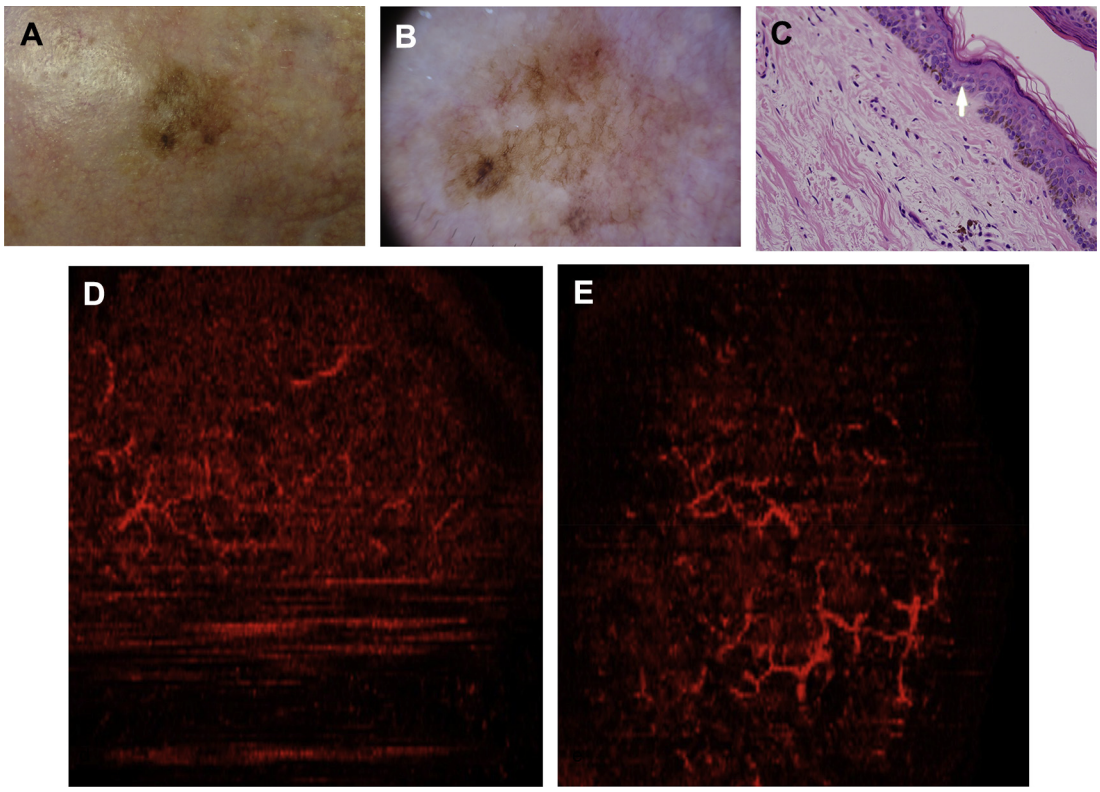

Fig. 5. Clinical, dermoscopy, histology an MM in situ on the forehead (*A–C*). En face D-OCT of a benign nevus (*D*) and a melanoma in situ (*E*). (*A*) Clinical image of melanoma in situ on the forehead, presented as a large, asymmetric pigmented lesion. (*B*) Dermoscopy shows asymmetric pigmented follicular opening, and slate gray dots and globules. (*C*) Corresponding histopathology (Haemotoxylin and Eosin). Arrow is pointing to the atypical melanocytes in the dermal-epidermal junction. (*D*) Benign nevi show regularly distributed vessels, comparable with the surrounding normal skin. (*E*) Melanoma in situ exhibit long linear vessels that appear broken and irregular and have a chaotic distribution.

had a stretching effect (see **Figs. 9** and **10**).[18] BCC subtypes can be differentiated by the vascular patterns that they display, as nBCCs are characterized by small, branched vessels, whereas iBCCs exhibit large, branched holes.[18]

Squamous Cell Carcinoma/Actinic Keratosis

On cross-sectional (vertical) sections, most AKs displayed a clear DEJ outline. In contrast, SCCs displayed irregular reflective buddings projecting from the epidermis deep into the dermis,

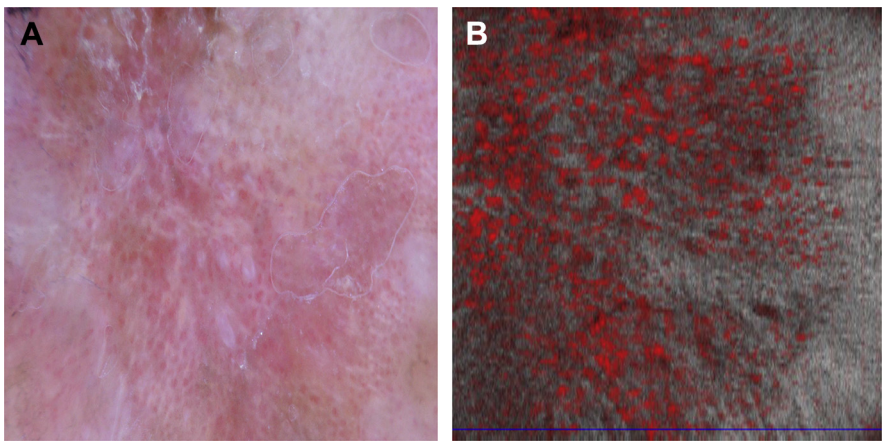

Fig. 6. Dermoscopy and en face D-OCT image of SCC. (*A*) Dermoscopy of SCC with small, dotted, and glomerular vessels distributed in packed clusters. (*B*) En-face D-OCT of SCC shows that vessels appear dotted in morphology.

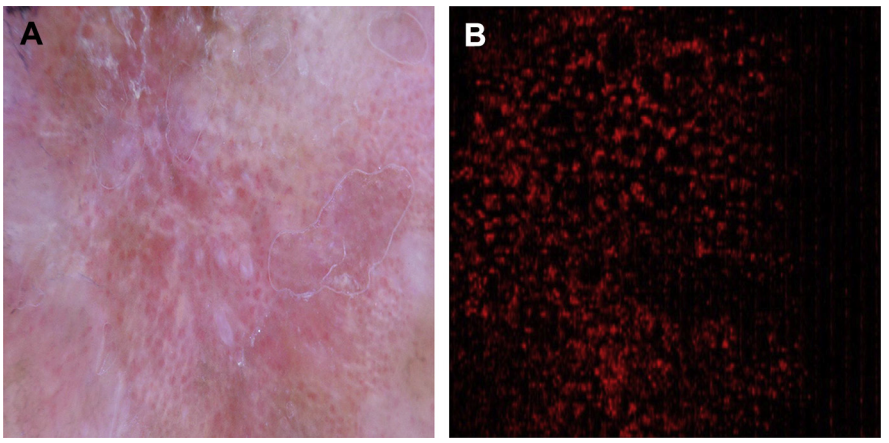

Fig. 7. Dermoscopy and en face D-OCT image of SCC. (*A*) Dermoscopy of SCC with small, dotted, and glomerular vessels distributed in packed clusters. (*B*) En-face D-OCT of SCC shows that vessels appear dotted in morphology similar to what is seen on dermoscopy.

interrupting or obscuring the DEJ.[22–24] All SCCs and AKs had alternating hyperkeratosis and parakeratosis as well as alternating atrophy and hypertrophy.[22–24]

On en face HD-OCT, the extent of disruption of the honeycomb pattern in the epidermis was found to correlate with the severity of AK and the diagnosis of SCC. A mildly atypical honeycomb pattern was displayed in most AKs, whereas a severely atypical honeycomb pattern was seen in 100% of SCCs.[22–24] In addition, about 50% of AKs and all SCCs had adnexal involvement, where the classic *cocarde* image (perifollicular hyporeflective band surrounded by a thin dark ring) was replaced by atypical keratinocytes cuffing the hair follicle.[22–24] This finding is significant as studies have shown that AKs with follicular extension have an increased risk of developing into SCCs (**Figs. 11** and **12**).[23]

Malignant Melanoma

Because of higher cellular resolution, HD-OCT has been found to have a higher diagnostic potential in differentiating between benign and malignant melanocytic lesions compared with FD-OCT.

Cellular findings of MM on cross-sectional HD-OCT include atypical large roundish pagetoid cells, junctional and/or dermal nests with atypical cell clusters, altered DEJ, and irregular and broadened rete ridges.[25–27]

Findings on en face mode include the following: superficial layer showed cobblestone or irregular honeycomb pattern; epidermal disarray observed

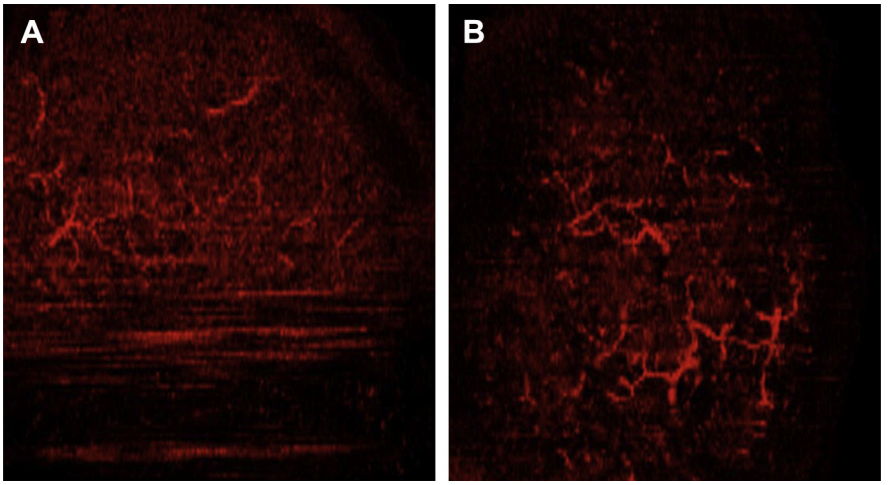

Fig. 8. En face D-OCT of a benign nevus and a melanoma in situ. (*A*) Benign nevi show regularly distributed vessels similar to the surrounding normal skin. (*B*) Melanomas in situ exhibit long linear vessels that appear broken and irregular and have a chaotic distribution that comprises the entire en face FOV.

Table 4
Summary of studies investigating the use of optical coherence tomography to evaluate skin cancers: dynamic optical coherence tomography/speckle-variance optical coherence tomography

First Author, Year, Country	Population Characteristics	Lesions, Number	Accuracy	Findings/Results	Limitations
Ulrich et al,[15] 2016, Germany	NR	NR	NR	Superficial BCC: cross-sectional view: progressive elongation of perpendicular vessel columns; en face view: variation in the calibers of the blood vessels, disorganized with a multitude of minute vessels AK: D-OCT: reticular network on en face view, which resembles the network of normal skin but vessels form a larger caliber and a slightly irregular, broader network Bowens/SCCIS: enface view: vessels appear dotted or semicircular Melanoma: densely clustered red dots may be visible in the superficial dermis; red dots aggregate to linear structures with increase in tumor thickness	NR
Markowitz et al,[16] 2016, United States	NR	4 lesions (sebaceous hyperplasia, BCC, MM in situ, pigmented AK)	NR	En face: BCC: had a focal vascular pattern with an erratic vascular organization compared with benign sebaceous tumor Normal telangiectasia with minimal focal vascular irregularity with pigmented AK MMIS: revealed diffuse thin irregular vessels dispersed throughout the entire field	Case series
De Carvalho et al,[17] 2016, Italy	NR	1		Benign lentiginous: Cross-section: thin regular columns on transversal section, and regularly distributed dots or short curved lines, progressively assuming a regular reticulated architecture with depth in en face view; did not differ from the vascular pattern of normal surrounding skin Melanoma: Cross-sectional: vessels organized in larger vertical columns, irregularly distributed En face: vascular pattern characterized by numerous densely packed dots progressively becoming irregular cloudlike structures with depth CD31 staining confirmed the correspondence of SV-OCT images	1 patient

Abbreviations: NR, not reported; SCCIS, SCC in situ.

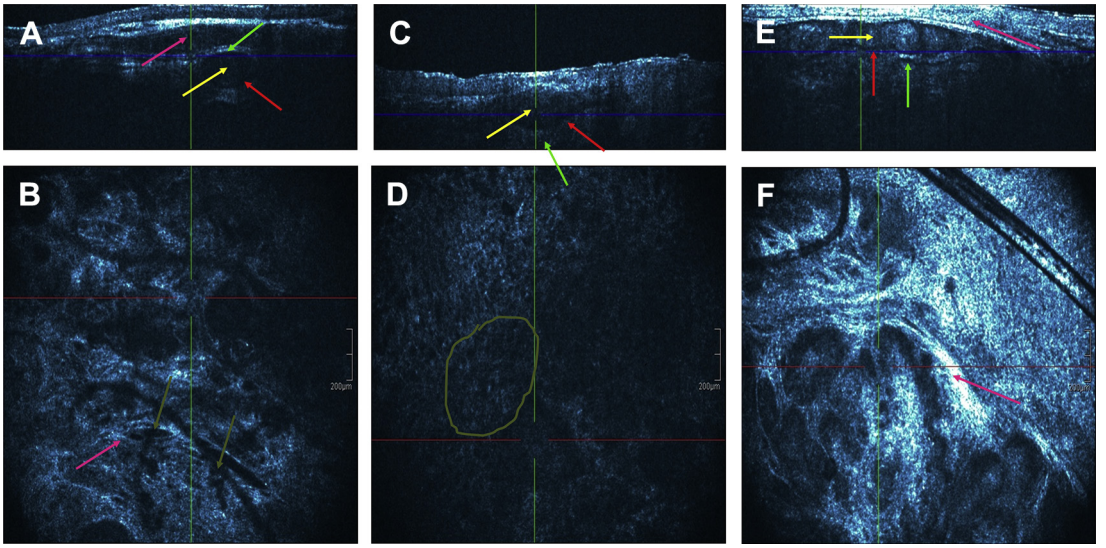

Fig. 9. HD-OCT features of infiltrative, sBCC, and nodular BCC. (*A*, *B*) Infiltrative BCC. Elongated, gray to black lobular structures can be observed, separated with deeper dermal localization and more pronounced stretching effect (*pink arrow*). The typical cockade image is present: the gray core (*yellow arrow*) of the lobular structure surrounded by the dark inner layer (*red arrow*) and bright peripheral outer rim (*green arrow*). There is an abundant of large, dilated branched vessels observed (*dark green arrow*). (*C*, *D*) sBCC. A hemispherical nestlike, dark-gray structure connected to the epidermis on cross-sectional images. Notice the increased and altered microvasculature (*dark green encircled area*). (*E*, *F*) Nodular BCC. Intradermal gray to dark colored structures with typical cockade feature present: a gray core (*yellow arrow*), an inner dark rim (*red arrow*), and an outer peripheral bright rim (*light green arrow*). These lobules cause abnormal dermal architecture in both cross-sectional and en face images. There is a stretching effect of the tumor on the fibrous structures, appearing as variably reflective stroma, located between lobular structures (*pink arrow*). (*Courtesy of* Mark Boone, MD, Lennik, Belgium.)

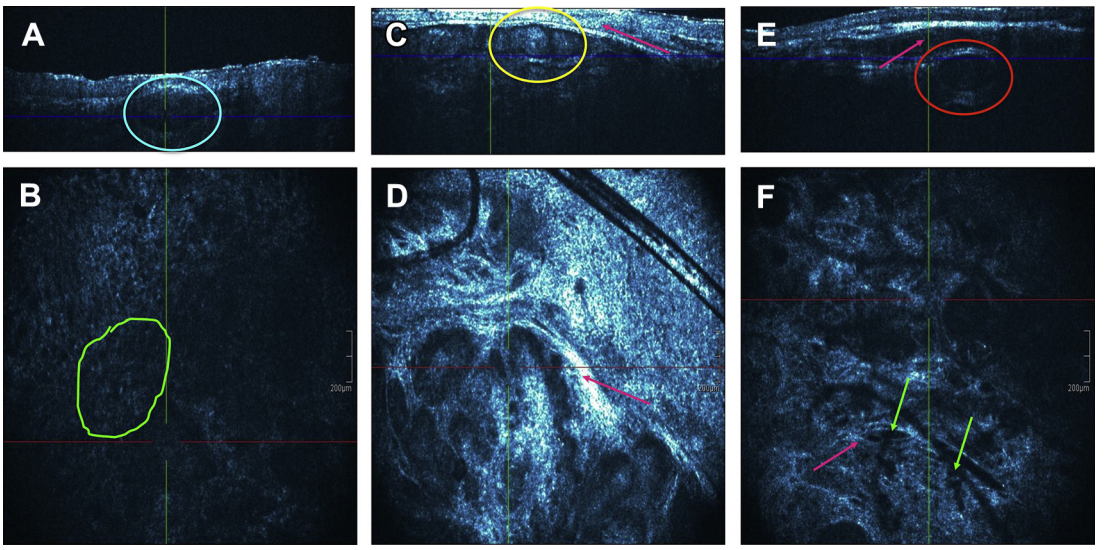

Fig. 10. HD-OCT features of sBCC, nodular, and infiltrative BCC. (*A*, *B*) sBCC. A hemispherical nestlike, dark-gray structure connected to the epidermis on cross-sectional images (*blue circle*). Notice the increased and altered microvasculature (*green encircled area*). (*C*, *D*) Nodular BCC. Intradermal gray to dark colored structures with typical cockade feature present: a gray core, an inner dark rim, and an outer peripheral bright rim (*yellow circle*). These lobules cause abnormal dermal architecture in both cross-sectional and en face images. There is a stretching effect of the tumor on the fibrous structures, appearing as variably reflective stroma, located between lobular structures (*pink arrow*). (*E*, *F*) Infiltrative BCC. Elongated, gray to black lobular structures can be observed, separated with deeper dermal localization and more pronounced stretching effect (*pink arrow*). The typical cockade image is present (*red circle*): the gray core of the lobular structure surrounded by the dark inner layer and bright peripheral outer rim. There is an abundant of large, dilated, branched vessels observed (*green arrows*). (*Courtesy of* Mark Boone, MD, Lennik, Belgium.)

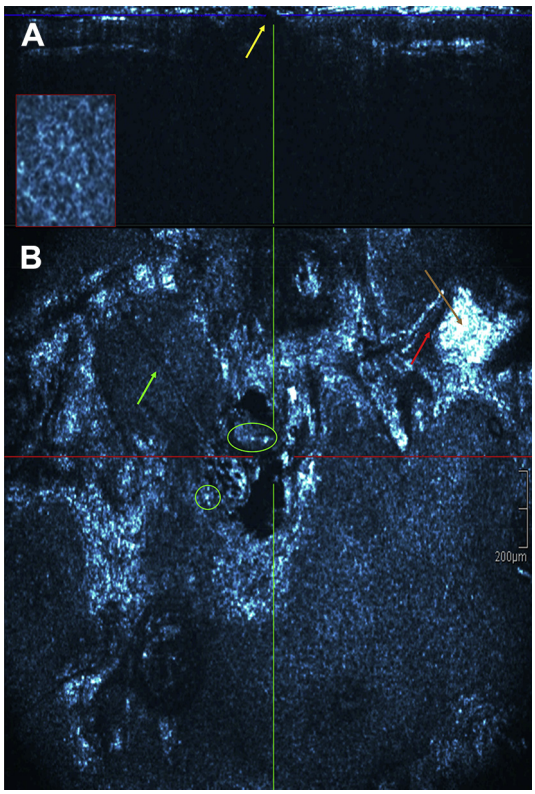

Fig. 11. Non-Bowenoid AK with adnexal involvement. Cross-sectional and en face HD-OCT image of AK with adnexal involvement. (*A*) In the cross-sectional mode, a follicular structure (*yellow arrow*) interrupts the subepidermal dark band. (*B*) In the en face view, you can see repression of normal adnexal epithelium by atypical cells, leading to the disa - ppearance of the classic cocarde image, which is replaced by atypical keratinocytes cuffing the hair follicle (hair follicle, *green arrow*; atypical cells, *green circle*). The borders of keratinocytes comprising the mildly atypical honeycomb pattern are more irregular and brighter and contours of nuclei are more masked (*close-up*). Notice the alternating hyperkeratosis (*red arrow*) with parakeratosis (*brown arrow*) that can be seen in both views. (*Courtesy of* Mark Boone, MD, Lennik, Belgium.)

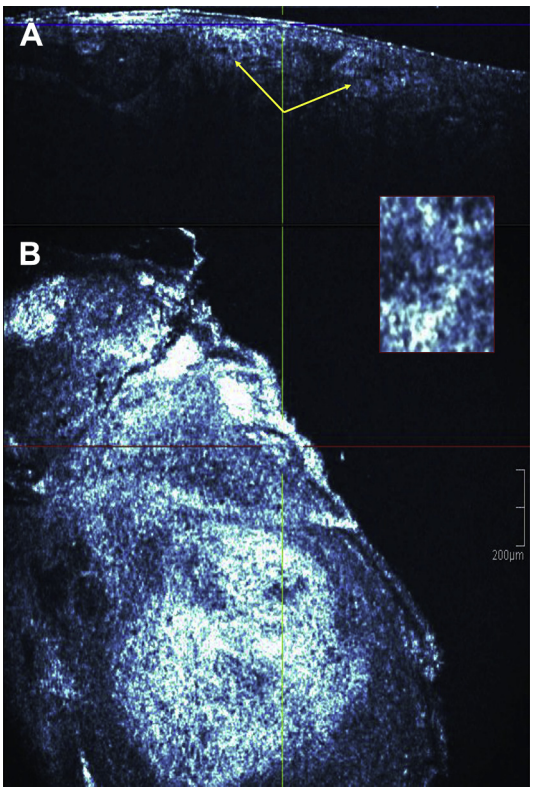

Fig. 12. Cross-sectional and en face HD-OCT image of SCC. (*A*) Cross-sectional HD-OCT image of an SCC. Notice the irregular budding of epidermis deeper into the dermis, obscuring the DEJ (*yellow arrows*). (*B*) En face HD-OCT of an SCC shows severe architectural disarray of the epidermis and dermis. Severely atypical honeycomb pattern (*close-up*). The DEJ is no longer present. Acantholysis is pronounced. (*Courtesy of* Mark Boone, MD, Lennik, Belgium.)

in areas of pagetoid spread; atypical melanocytes observed in the upper part of dermis (**Figs. 13** and **14**).[25–27]

LIMITATIONS

Two cases of amelanotic melanomas being misdiagnosed as BCCs on FD-OCT have been reported.[7,8,28] Clinicians must remain cautious about using this modality to assist noninvasive diagnosis of clinically uncertain amelanotic or hypomelanotic skin lesions because some OCT features are nonspecific and overlap with amelanotic melanomas.[7,8,28] Further studies need to be done to see if D-OCT can help to differentiate this.

Olsen and colleagues[10] and Wahrlich and colleagues[29] used FD-OCT to show that both experts and nonexperts overdiagnosed NMSC lesions resulting in a high sensitivity but only an average specificity. This finding is thought to be because the OCT images of healthy skin were obtained from skin next to NMSC lesions and, therefore, likely had features of sun damage due to field cancerization.[10,29]

Gambichler and colleagues[27] demonstrated a limitation for HD-OCT in melanoma diagnosis in that accuracy depends on tumor thickness and the presence of borderline lesions. In their study, this is indicated by a high false-negative rate in very thin melanomas and a high false-positive rate in dysplastic nevi, making it still inferior to RCM.[27]

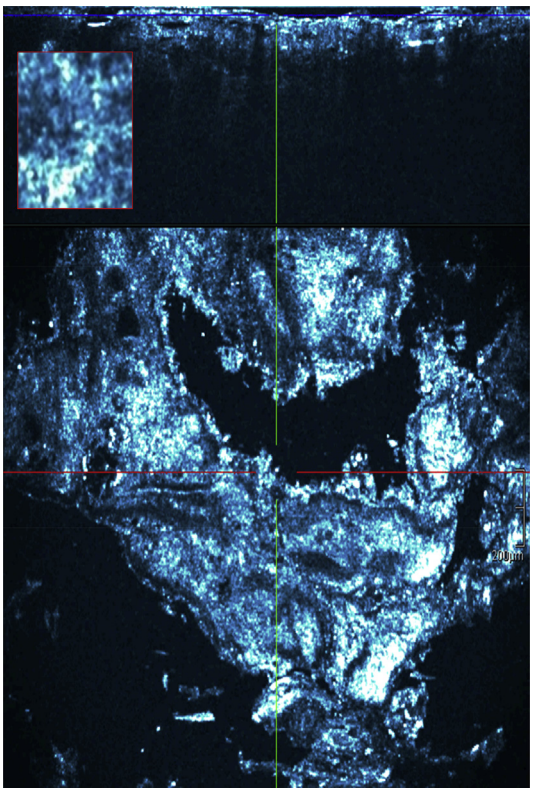

Fig. 13. Bowenoid AK. Cross-sectional (slice) and en face HD-OCT images. This lesion represents a carcinoma in situ with full- thickness atypia involving the epidermis and adnexal structures. A complete disarranged epidermal pattern and acantholysis are observed. (*Courtesy of* Mark Boone, MD, Lennik, Belgium.)

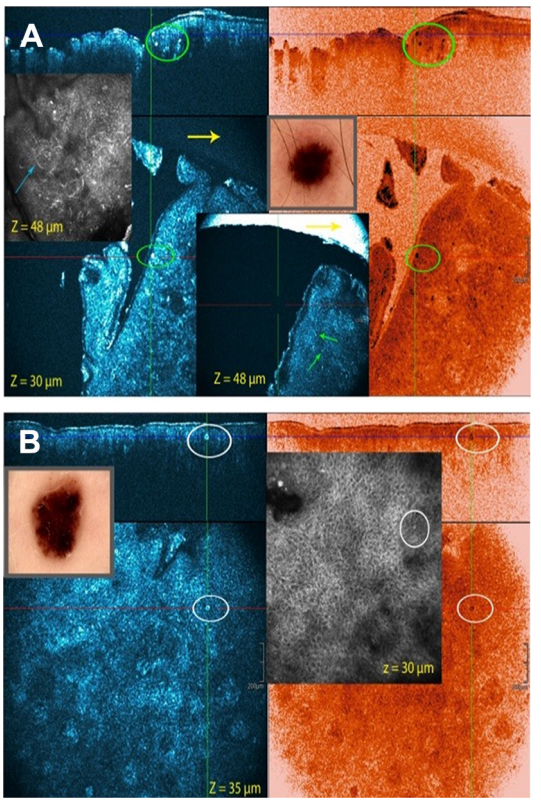

Fig. 14. Pagetoid melanoma. (*A*, *B*) Pagetoid melanocytosis is represented by the presence of large melanocytes (twice the size of neighboring keratinocyte) with abundant reflective cytoplasm (*green circle*) and sometimes characterized by a prominent hyporeflective nucleus depending on the image focus (*white circle*). (*A*) The pagetoid cells may be more elongated with variable morphology of the branches. Thick branches can be observed by HD-OCT (*green arrow*). Thin, bright filamentous structures are only observed by RCM (*blue arrow*). On the HD-OCT en face images, the 2-mm diameter plastic ring can be observed (*yellow arrow*). (*Courtesy of* Mark Boone, MD, Lennik, Belgium.)

All noninvasive imaging devices were limited as a result of increased lesion thickness; therefore, clinically apparent lesions, such as hypertrophic AKs, lead to difficulty in visualizing the deeper structures.[23,24] This difficulty was even an issue with FD-OCT, despite its increased depth.

MONITORING OF SURGICAL AND NONSURGICAL SKIN CANCER THERAPIES

With the advent of new nonsurgical therapeutic options for NMSC, such as topical chemotherapy, immunomodulators, and photodynamic therapy, noninvasive imaging is useful in the monitoring of treatment progress as well as determining treatment efficacy.[30–33] Noninvasive treatment monitoring is also useful in patients with lesions on cosmetically sensitive areas of the face, as these patients often refuse posttreatment biopsy confirmation.

An additional use specific to all OCT devices is defining tumor margins before surgery. Studies have shown that the OCT margin was always on or within the clinical defect boundary.[34–37] Delineating tumor margins preoperatively can potentially reduce the number of stages required.[34–37]

SUMMARY

OCT is a noninvasive imaging technique that produces highly sensitive and specific images of tissue microstructure. This ability allows for improved diagnostic accuracy for a variety of both benign and malignant skin conditions. FD-OCT, D-OCT, and HD-OCT are the main devices reviewed in this article; all have been shown to be useful for NMSCs and precancerous growths. More research is currently being done to understand the role of these devices with pigmented lesions in differentiating melanoma. Other unique

benefits of OCT given its depth and broader FOV are both monitoring lesion treatment undergoing nonsurgical therapy and in delineating margins before surgery.

ACKNOWLEDGEMENTS

The authors would like to thank Marc Boone, MD for contributing the HD-OCT images.

REFERENCES

1. Schwartz M, Siegel D, Markowitz O. Commentary on the diagnostic utility of non-invasive imaging devices for field cancerization. Exp Dermatol 2016; 25:855–6.
2. Schmitz L, Reinhold U, Bierhoff E, et al. Optical coherence tomography: its role in daily dermatological practice. J Dtsch Dermatol Ges 2013; 11(6):499–507.
3. Gambichler T, Jaedicke V, Terras S. Optical coherence tomography in dermatology: technical and clinical aspects. Arch Dermatol Res 2011;303:457–73.
4. Gambichler T, Pljaki A, Schmitz L. Recent advances in clinical application of optical coherence tomography of human skin. Clin Cosmet Investig Dermatol 2015;8:345–54.
5. Jemef GB, Gniadecka M, Ulrich J. Ultrasound in dermatology. Part I. High frequency ultrasound. Eur J Dermatol 2000;10:492–7.
6. Markowitz O, Schwartz M, Feldman E, et al. Evaluation of optical coherence tomography as a means of identifying earlier stage basal cell carcinomas while reducing the use of diagnostic biopsy. J Clin Aesthet Dermatol 2015;8(10):14–20.
7. Ulrich M, von Braunmuehl T, Kurzen H, et al. The sensitivity and specificity of optical coherence tomography for the assisted diagnosis of nonpigmented basal cell carcinoma: an observational study. Br J Dermatol 2015;173(2):428–35. Available at: https://www.ncbi.nlm.nih.gov/PubMed/25904111.
8. Cheng HM, Lo S, Scolyer R, et al. Accuracy of optical coherence tomography for the diagnosis of superficial basal cell carcinoma: a prospective, consecutive, cohort study of 168 cases. Br J Dermatol 2016;175(6):1290–300.
9. Meekings A, Utz S, Ulrich M, et al. Differentiation of basal cell carcinoma subtypes in multi-beam swept source optical coherence tomography (MSS-OCT). J Drugs Dermatol 2016;15(5):545–50.
10. Olsen J, Themstrup L, De Carvalho N, et al. Diagnostic accuracy of optical coherence tomography in actinic keratosis and basal cell carcinoma. Photodiagnosis Photodyn Ther 2016;16:44–9.
11. Hussain A, Themstrup L, Jemec GBE. Optical coherence tomography in the diagnosis of basal cell carcinoma. Arch Dermatol Res 2015;307:1–10.
12. Maier T, Cekovic D, Ruzicka T, et al. Treatment monitoring of topical ingenol mebutate in actinic keratoses with the combination of optical coherence tomography and reflectance confocal microscopy: a case series. Br J Dermatol 2015;172(3):816–8.
13. Blumetti T, Cohen M, Gomes E, et al. Optical coherence tomography (OCT) features of nevi and melanomas and their association with intraepidermal or dermal involvement: a pilot study. J Am Acad Dermatol 2015;73(2):315–7.
14. Gambichler T, Regeniter P, Bechara F, et al. Characterization of benign and malignant melanocytic skin lesions using optical coherence tomography in vivo. J Am Acad Dermatol 2007;57(4):629–37.
15. Ulrich M, Themstrup L, de Carvalho N, et al. Dynamic optical coherence tomography in dermatology. Dermatology 2016;232:298–311.
16. Markowitz O, Schwartz M, Minhas S, et al. Speckle-variance optical coherence tomography: a novel approach to skin cancer characterization using vascular patterns. Dermatol Online J 2016;22(4) [pii:13030/qt7w10290r].
17. De Carvalho N, Ciardo S, Cesinaro AM, et al. In vivo micro-angiography by means of speckle-variance optical coherence tomography (SV-OCT) is able to detect microscopic vascular changes in nevus to melanoma transition. J Eur Acad Dermatol Venereol 2015;30:e29–108.
18. Boone M, Suppa M, Pellacani G, et al. High-definition optical coherence tomography algorithm for discrimination of basal cell carcinoma from clinical BCC imitators and differentiation between common subtypes. J Eur Acad Dermatol Venereol 2015;29: 1771–80.
19. Li G, Tietze JK, Tao X, et al. High-definition optical coherence tomography in the diagnosis of basal cell carcinoma evaluated by an experienced versus inexperienced investigator. Clin Exp Dermatol Res 2014;5:4.
20. Gambichler T, Plura I, Kampilafkos P, et al. Histopathological correlates of basal cell carcinoma in the slice and en face imaging modes of high-definition optical coherence tomography. Br J Dermatol 2014;170:1358–61.
21. Maier T, Braun-Falco M, Hintz T, et al. Morphology of basal cell carcinoma in high definition optical coherence tomography: en-face and slice imaging mode, and comparison with histology. J Eur Acad Dermatol Venereol 2013;27(1):e97–104.
22. Malvehy J. A new vision of actinic keratosis beyond visible clinical lesions. J Eur Acad Dermatol Venereol 2015;29(1):3–8.
23. Boone MA, Marneffe A, Suppa M, et al. High-definition optical coherence tomography algorithm for the discrimination of actinic keratosis from normal skin and from squamous cell carcinoma. J Eur Acad Dermatol Venereol 2015;29:1606–15.

24. Marneffe A, Suppa M, Miyamoto M, et al. Validation of a diagnostic algorithm for the discrimination of actinic keratosis from normal skin and squamous cell carcinoma by means of high-definition optical coherence tomography. Exp Dermatol 2016;25:684–7.
25. Gambichler T, Schmid-Wendtner MH, Plura I, et al. A multicenter pilot study investigating high-definition optical coherence tomography in the differentiation of cutaneous melanoma and melanocytic nevi. J Eur Acad Dermatol Venereol 2015;29(3):537–41.
26. Boone M, Norrenberg S, Jemec G, et al. High-definition optical coherence tomography imaging of melanocytic lesions: a pilot study. Arch Dermatol Res 2014;306:11–26.
27. Gambichler T, Plura I, Schmid-Wendtner MH, et al. High-definition optical coherence tomography of melanocytic skin lesions. J Biophotonics 2014;8(8):681–6.
28. Maher NG, Blumetti TP, Gomes EE, et al. Melanoma diagnosis may be a pitfall for optical coherence tomography assessment of equivocal amelanotic or hypomelanotic skin lesions. Br J Dermatol 2016. [Epub ahead of print].
29. Wahrlich C, Alawi SA, Batz S, et al. Assessment of a scoring system for basal cell carcinoma with multibeam optical coherence tomography. J Eur Acad Dermatol Venereol 2015;29:1562–9.
30. Markowitz O, Schwartz M, Feldman E, et al. Defining field cancerization of the skin using noninvasive optical coherence tomography imaging to detect and monitor actinic keratosis in ingenol mebutate 0.015%-treated patients. J Clin Aesthet Dermatol 2016;9(5):18–25.
31. Banzhaf C, Themstrup L, Ring H, et al. Optical coherence tomography imaging of non-melanoma skin cancer undergoing imiquimod therapy. Skin Res Technol 2014;20:170–6.
32. Themstrup L, Banzhaf CA, Mogensen M, et al. Optical coherence tomography imaging of non-melanoma skin cancer undergoing photodynamic therapy reveals subclinical residual lesions. Photodiagnosis Photodyn Ther 2014;11:7–12.
33. Hussain AA, Themstrup L, Nurnberg BM, et al. Adjunct use of optical coherence tomography increases the detection of recurrent basal cell carcinoma over clinical and dermoscopic examination alone. Photodiagnosis Photodyn Ther 2016;14:178–84.
34. Alawi SA, Kuck M, Wahrlich C, et al. Optical coherence tomography for presurgical margin assessment of non-melanoma skin cancer- a practical approach. Exp Dermatol 2013;22:547–51.
35. Wang KX, Meekings A, Fluhr JW, et al. Optical coherence tomography-based optimization of Mohs micrographic surgery of basal cell carcinoma: a pilot study. Dermatol Surg 2013;39:627–33.
36. Coleman AJ, Penney GP, Richardson TJ, et al. Automated registration of optical coherence tomography and dermoscopy in the assessment of sub-clinical spread in basal cell carcinoma. Comput Aided Surg 2014;19:1–12.
37. Mogensen M, Joergensen TM, Nürnberg BM, et al. Assessment of optical coherence tomography imaging in the diagnosis of non- melanoma skin cancer and benign lesions versus normal skin: observer-blinded evaluation by dermatologists and pathologists. Dermatol Surg 2009;35:965–72.